JOURNAL OF VIROLOGY, Nov. 2004, p. 12406–12415 Vol. 78, No. 22
0022-538X/04/$08.00+0 DOI: 10.1128/JVI.78.22.12406–12415.2004

Functions of the C-Terminal Domain of Varicella-Zoster Virus Glycoprotein E in Viral Replication In Vitro and Skin and T-Cell Tropism In Vivo

Jennifer Moffat,[1]* Chengjun Mo,[2]† Jason J. Cheng,[2]‡ Marvin Sommer,[2] Leigh Zerboni,[2] Shaye Stamatis,[2] and Ann M. Arvin[2]

Department of Microbiology and Immunology, State University of New York Upstate Medical University, Syracuse, New York,[1] and Departments of Pediatrics and Microbiology and Immunology, Stanford University, Stanford, California[2]

Received 14 January 2004/Accepted 30 June 2004

Varicella-zoster virus (VZV) glycoprotein E (gE) is essential for VZV replication. To further analyze the functions of gE in VZV replication, a full deletion and point mutations were made in the 62-amino-acid (aa) C-terminal domain. Targeted mutations were introduced in YAGL (aa 582 to 585), which mediates gE endocytosis, AYRV (aa 568 to 571), which targets gE to the *trans*-Golgi network (TGN), and SSTT, an "acid cluster" comprising a phosphorylation motif (aa 588 to 601). Substitutions Y582G in YAGL, Y569A in AYRV, and S593A, S595A, T596A, and T598A in SSTT were introduced into the viral genome by using VZV cosmids. These experiments demonstrated a hierarchy in the contributions of these C-terminal motifs to VZV replication and virulence. Deletion of the gE C terminus and mutation of YAGL were lethal for VZV replication in vitro. Mutations of AYRV and SSTT were compatible with recovery of VZV, but the AYRV mutation resulted in rapid virus spread in vitro and the SSTT mutation resulted in higher virus titers than were observed for the parental rOka strain. When the rOka-gE-AYRV and rOka-gE-SSTT mutants were evaluated in skin and T-cell xenografts in SCIDhu mice, interference with TGN targeting was associated with substantial attenuation, especially in skin, whereas the SSTT mutation did not alter VZV infectivity in vivo. These results provide the first information about how targeted mutations of this essential VZV glycoprotein affect viral replication in vitro and VZV virulence in dermal and epidermal cells and T cells within intact tissue microenvironments in vivo.

Varicella-zoster virus (VZV) is an alphaherpesvirus with a genome of ~125,000 bp, encoding at least 70 unique open reading frames (ORFs) (3, 8, 10). Primary VZV infection causes varicella, which is characterized by cell-associated viremia and the formation of vesicular skin lesions that contain high concentrations of cell-free virions (3, 19, 35). It is believed that VZV is transmitted by aerosolized virions and infected cell material shed from skin and respiratory epithelium, although this process has not been tested in animal models. VZV preferentially infects memory T cells that have skin homing markers, as a mechanism for its transfer from respiratory epithelial sites of inoculation to dermal and epidermal cells (19). VZV establishes latency in sensory ganglia and causes herpes zoster upon reactivation. Thus, VZV pathogenesis requires infection of circulating lymphocytes, skin, and neural cells. The highly cell-associated nature of VZV replication in vitro and its very restricted infectivity in nonhuman species have been obstacles to understanding how viral gene products contribute to VZV replication and to the infection of specific target cells that are important for the viral life cycle in the host. Two advances have provided new opportunities to analyze the molecular mechanisms of VZV infectivity in vitro and in vivo. First, the use of VZV cosmids permits the identification of VZV genes, or regions within the coding sequence for particular viral proteins, that are required for viral replication in cell culture (7, 16, 20). When changes in the VZV genome are compatible with viral growth in vitro, VZV recombinant viruses with targeted mutations of viral genes or their promoters can be generated to map critical functions. Second, the SCIDhu mouse model, in which human skin and T-cell xenografts are infected in vivo, makes it possible to define the effects of nonlethal VZV mutations on virulence in these differentiated human cells within their unique tissue microenvironments (4, 6, 14, 24–27, 32–34).

Glycoprotein E (gE), a 623-amino-acid (aa) type I integral membrane protein, is expressed on plasma membranes and in the cytoplasm of VZV-infected cells, where it is presumed to be present in the membranes of intracellular vesicles or organelles (8). VZV gE complexes with gI in the rough endoplasmic reticulum, and most gE exists in the form of gE-gI heterodimers in infected cells (1, 2, 9, 18, 39–41). VZV gE is also a predominant component of the virion envelope. The functions of gE, which is encoded by ORF68, are of particular interest because it has been demonstrated that ORF68 is essential for VZV replication (22). In contrast, the genes for gE proteins can be deleted from herpes simplex virus and pseudorabies virus, albeit with significant reductions in infectivity in cell culture and in animal models (5, 11, 15, 37). Since the VZV genome does not encode a homologue of gD, VZV gE

* Corresponding author. Mailing address: Department of Microbiology and Immunology, SUNY Upstate Medical University, 750 East Adams St., Syracuse, NY 13210. Phone: (315) 464-5454. Fax: (315) 464-4417. E-mail: moffatj@upstate.edu.

† Present address: MedImmune Vaccines, Inc., Mountain View, Calif.

‡ Present address: University of California at San Francisco School of Medicine, San Francisco, Calif.

may have functions that are usually segregated between gD and gE, or the gE-gI complex, in other alphaherpesviruses.

VZV gE is predicted to be important for mediating cell-cell spread of the virus as well as for the assembly of intact enveloped virions. Endocytosis of gE is facilitated by gI, and gI regulates the trafficking of the gE-gI complex (29, 30, 40). VZV gE enhances cell-cell contact in polarized epithelial cells, with or without gI expression (23). VZV mutants that have full or partial deletions of gI can replicate, but they exhibit small plaques, aberrant syncytium formation, abnormal gE trafficking and maturation, and decreased production of infectious virus in vitro (7, 14, 16). While gI is dispensable in vitro in MeWo cells and primary fibroblasts, one gI deletion mutant was unable to replicate in Vero cells (7). On the other hand, gI expression is necessary for VZV infection of skin and T-cell xenografts in the SCIDhu model, demonstrating that gE-gI interactions are essential for VZV virulence in differentiated host cells in vivo (24). VZV gE and gE-gI interactions may be required for production of enveloped infectious virions through interactions with tegument proteins in the *trans*-Golgi network (TGN) (22, 30). VZV gE has targeting sequences for the TGN in its C terminus, and it is transported from the endoplasmic reticulum (ER) to the TGN in infected and gE-transfected cells (12, 40). Most gE in the TGN appears to be retrieved by endocytosis from plasma membranes and delivered to the TGN by endosomes, followed by recycling to plasma membranes (1, 12, 29, 30, 39). Accumulation of gE in the TGN, along with tegument proteins, such as ORF10 protein, is associated with the production of fully enveloped VZV virions in vitro (40).

The purpose of these experiments was to examine the functions of gE by mutagenesis of ORF68 in the context of the VZV genome and to evaluate the consequences for replication in vitro and for VZV virulence in skin and T-cell xenografts in vivo. We focused on the contributions of residues in the C terminus of gE, which constitutes its small, 62-aa endodomain. By using transient expression methods, two functional motifs have been identified within the gE C-terminal domain. An AYRV sequence (aa 568 to 571) is required for targeting of gE to the TGN, as shown by disrupted sorting when mutant gE was expressed from the gE-Y569A plasmid (41). The AYRV motif may function to shuttle new gE molecules from the Golgi appararus to the TGN. A YAGL sequence (aa 582 to 585), resembling other YXXL endocytosis motifs, mediates gE internalization when gE is expressed transiently in HeLa cells. Changing Y to G in the gE-Y582G plasmid prevented gE endocytosis (29). The cytoplasmic tail of gE also contains an "acid patch," a cluster of acidic amino acids, including two serines (S593 and S595) and two threonines (T596 and T598) (17). These residues are differentially phosphorylated by the VZV ORF47 protein kinase, which targets all four amino acids, and cellular casein kinase II (CKII), which preferentially phosphorylates the threonines. gE localization to the TGN was reduced in the absence of ORF47 kinase activity, suggesting that phosphorylation of these residues by the viral kinase was necessary for correct gE trafficking.

Using cosmids derived from DNA of the VZV vaccine strain Oka, we deleted the gE C-terminal domain and generated targeted mutations in ORF68 that changed the YAGL endocytosis motif to GAGL, altered the AYRV TGN localization motif to AARV, or replaced the serines and threonines in the SSTT acidic cluster with alanines. These experiments demonstrated that the C terminus of gE and the YAGL motif were necessary for VZV replication. The AYRV motif was not essential in vitro but was required for efficient replication, particularly in skin, in vivo. Disrupting the serine and threonine phosphorylation targets of the ORF47 and CKII kinases did not affect VZV replication in vitro or its virulence in skin or T cells in vivo.

MATERIALS AND METHODS

Cells and viruses. Recombinant VZV Oka (rOka) and the gE C-terminal mutants were derived from cosmids according to previously described methods (20). Viruses were propagated in human melanoma cells (strain MeWo), Vero cells, or primary human epithelial lung (HEL) cells (25, 36). MeWo cells are highly permissive for VZV replication, with no release of infectious virus into the culture medium (13).

Construction of plasmids and cosmids. Deletion of the C terminus of gE was done with primers designed to amplify the sequence encoding the gE N terminus and the transmembrane domain, consisting of aa 1 to 561, by using pLITMUS ORF66-68 as the template (22). The primers were ΔgE-C (5′-TGATCACCGA ACCGGGGCAAC-3′), which anneals at VZV nucleotide 117677, and gEΔC (5′-TGAAGCCGTACAGATTAAAAATA-3′), which anneals at nucleotide 117490. The PCR product was gel purified and ligated to generate pLITMUS ORF66-68 gEΔC. After AatII/AvrII digestion and gel purification, a 5.7-kb DNA fragment from pLITMUS ORF66-68 gEΔC and a 12.5-kb DNA fragment from pLITMUS28/VZV were ligated to yield pLITMUS28/VZVgEΔC. Spe21ΔTRs (12) and pLITMUS28/VZVgEΔC were digested with AvrII/SrfI, and the 16.5-kb fragment from Spe21ΔTRs and the 10.8-kb fragment from pLITMUS28/VZVgEΔC were ligated to generate Spe21ΔTRs/gEΔC. Spe21ΔTRs/gEΔC was digested with AvrII/NheI; the 15.4-kb fragment was isolated and ligated to the 21.2-kb fragment of Spe21ΔAvrII generated by the AvrII/NheI cleavage to produce Spe21gEΔC.

Three plasmids, pLITMUS66-68 SSTT, pLITMUS66-68 AYRV, and pLITMUS66-68 YAGL, which encoded the indicated site-directed mutation in the gE C terminus, were constructed by PCR mutagenesis using complementary and mutagenic oligonucleotides whose 5′ ends annealed to adjacent nucleotides on opposite DNA strands (Table 1). PCRs were performed with Elongase enzyme (Invitrogen, Grand Island, N.Y.) to synthesize the complete pLITMUS66-68 plasmid, incorporating point mutations in the gE C terminus. The PCR products were gel purified, phosphorylated by T4 kinase (New England Biolabs, Inc.), and ligated to produce circular plasmids that were subsequently electroporated into *Escherichia coli*. Alterations in the AYRV site created a new SstII restriction site and changed the amino acid sequence to AAGV. YAGL was changed to GAGL, creating a new NarI site, and SESTDT (SSTT) was changed to AEAADA, creating a new PvuII site. Plasmids were screened for mutations in ORF68, and positive clones were confirmed by sequencing.

The mutated ORF68 genes were introduced into pvSpe21ΔgE, the cosmid from which intact ORF68 had been deleted (12). Two PCR primers were designed to transfer the ORF68 point mutations into the pvSpe21ΔgE cosmid. Primer 1 anneals 279 nucleotides upstream of the ORF68 start codon and introduces an AvrII site. The primer sequence is 5′-CACATTCCCTAGGAAAC CCGTTTG-3′ (boldfaced nucleotides indicate the sites that were changed in order to introduce the AvrII site, which is underlined). Primer 2 anneals 229 nucleotides downstream of the ORF68 stop codon and introduces an AvrII site. The primer sequence is 5′-GCATCCGCGCCTAGGTATATGACC-3′. Templates for the PCRs were plasmids pLITMUS66-68 SSTT, pLITMUS66-68 AYRV, and pLITMUS66-68 YAGL. PCRs were carried out using Elongase enzyme. The 2.4-kb PCR products were isolated and cloned into the pCR-TOPO cloning vector (Invitrogen). Positive clones were sequenced to verify that the AvrII sites had been introduced and that the clones contained the expected ORF68 site mutation. To insert the mutated ORF68 gene into the cosmid, the TOPO vector containing the mutant ORF68 was digested with AvrII, and the 2.4-kb fragment containing ORF68 was isolated. Cosmid pvSpe21ΔgE was linearized with AvrII and dephosphorylated. The fragments that contained mutated ORF68 were ligated into the pvSpe21ΔgE vector. Ligated DNAs were electroporated into Top10F′ electrocompetent cells (Invitrogen) and grown in kanamycin and ampicillin. Clones were screened for the ORF68 insert; positive clones were sequenced to verify the ORF68 mutation.

Transfection, DNA isolation, and confirmation of mutations by PCR and

TABLE 1. Oligonucleotide primers used for PCR

Oligonucleotide	Sequence (5′→3′)[a]	Annealing site (5′ end)[b]
gEΔC up	TGATCACCGAACCGGGGCAAC	117677
gEΔC rev	TGAAGCCGTACAGATTAAAAATA	117490
	←D V **G** **A** A K V	
AYRVup	GTC TAC CC**C CGC GG**C TTT AAC	117523
	SstII	
AYRVrev	AAGTCCCCGTATAACCAAAGC	117524
	←L G A **G** Y M	
YAGLup	GG AAG GCC **GGC GCC** ATA CAT G	117564
	NarI	
YAGLrev	AGTGGACGATTTCGAGGACTC	117565
	D **A** E **A** **A** D **A** E E→	
SSTTlo	AG GAC **G**CG GAA **GCA GCT** GAT **G**CG GAA GAA G	117608
	PvuII	
SSTTrev	AGTTTGGTAACGCGATTGGAG	117609
AvrII-ORF68	CACATTC**CTAGG**AAACCCGTTTG	115529
	AvrII	
ORF68-AvrII	GCATCCGCG**CTAGG**TATATGACC	117899
	AvrII	
pgEf	AACTAATTATCCCGGATTTT	115561
pgEb	TCACCGGGTCTTATCTATAT	117679

[a] Altered bases and amino acids are boldfaced; arrows indicate direction of protein synthesis.
[b] VOka sequence, GenBank accession number NC_001348.

sequencing. Cosmid transfection and viral DNA isolation procedures were done as described previously (20, 22, 34). As described for analysis of the mutant cosmids, PCR was used to confirm the expected changes in DNA from recombinant viruses and to sequence the regions spanning the ORF68 mutations designed to alter the AYRV, YAGL, and SSTT residues.

Construction of gE-expressing cell lines. Met-gE cells were derived as described previously (22). Additional gE-expressing cell lines, designated pGlowgE cells, were made by amplifying ORF68, as well as 271 bp upstream and 183 bp downstream of ORF68, from pLITMUS ORF66-68 by using primers pgEf and pgEb (5′-AACTAATTATCCCGGATTTT-3′ and 5′-TCACCGGGTCTT ATC TATAT). The 2.3-kb PCR product was ligated into the pGlow vector (Invitrogen, Inc.). Orientation of the inserts was assessed by restriction enzyme digestion and verified by DNA sequencing. The pGlowgE plasmid, with the gE promoter sequence and the BGH-poly(A) sequence from the pGlow vector, was used to construct stably transfected pGlowgE MeWo cell lines. Human MeWo cells were grown in Dulbecco's minimal essential medium supplemented with 10% fetal calf serum, nonessential amino acids, penicillin-streptomycin, and amphotericin B. The pGlowgE plasmid was transfected into melanoma cells by using the Lipofectin method (Gibco BRL, Grand Island, N.Y.). After 4 weeks of selection in a medium containing 300 μg of G418/ml, the surviving clones were isolated and expanded for further screening. The presence of ORF68 was confirmed by PCR analysis of DNA extracted from pGlowgE cells. The pGlowgE cell lines were screened for gE expression by infecting them with vOka-MSPgE, which expresses a variant of gE that is not recognized by the anti-gE monoclonal antibody (MAb) 3B3 (32). Cells from ORF68-positive clones were seeded at 1×10^5 to 2×10^5 cells/well in 6-well plates; after 24 h, vOka-MSPgE-infected MeWo cells ($\sim 10^3$ cells/well) were added to each well. Infected pGlowgE cells were harvested after 48 h, protein lysates were separated on sodium dodecyl sulfate-polyacrylamide gel electrophoresis (SDS-PAGE) (10% polyacrylamide) gels, and Western blot analysis was carried out with MAb 3B3 to assess gE expression by the cell lines. Cells from the clone designated pGlowgE6 showed high gE expression after vOka-MSPgE infection and were expanded. The cell lines were used at a passage number of <10 for complementation experiments.

Growth kinetics and infectious focus assay. Growth curves were performed by using subconfluent MeWo cell monolayers in 6-well plates. The monolayers were inoculated on day 0 with cell-associated virus (approximately 5×10^3 PFU/well) and incubated at 37°C under 5% CO_2 for 6 days. Samples were harvested daily by collecting the supernatants and combining them with the adherent cells that had been dislodged with trypsin. The samples were centrifuged briefly to pellet the cells and then resuspended in exactly 1.0 ml of tissue culture medium. These cell suspensions were serially diluted 10-fold in tissue culture medium, and 0.1 ml was added to MeWo cell monolayers in 24-well plates in triplicate. When plaques were visible (4 to 6 days), the cells were fixed and stained with crystal violet in 3.7% formalin. Plaques were counted under a dissecting microscope (magnification, ×4), and the yield of infectious VZV per sample was calculated.

Confocal microscopy. MeWo or Vero cells were infected with rOka or rOka-gE mutant viruses. After 72 h, cells were fixed, permeabilized, and incubated with the anti-gE MAb 3B3 (kindly provided by Charles Grose, University of Iowa) and a rabbit anti-VZV IE62 polyclonal antibody. The epitope of MAb 3B3 is located in the gE N terminus between aa 149 and 161 (32). After a wash with phosphate-buffered saline (PBS)-bovine serum albumin (BSA), specimens were stained with the secondary antibodies, goat anti-mouse immunoglobulin G (IgG) conjugated with FITC (Jackson Immunoresearch, Inc.) and goat anti-rabbit IgG conjugated with Texas Red. In some experiments, cells were incubated with the anti-gE MAb and the fluorescent lipid Golgi apparatus marker C_6NBD-ceramide (50 nM) (Molecular Probes, Inc.), washed with PBS-BSA, and incubated with goat anti-mouse IgG conjugated with Texas Red; other experiments were done using a rabbit polyclonal antiserum against VZV glycoprotein I (14). Cells were examined with a Molecular Dynamics MultiProbe 2010 laser scanning confocal microscope.

To assess earlier changes, melanoma cells were grown on chamber slides (Nunc, Inc.), infected with rOka or rOka-gE C-terminal mutant viruses, and incubated at 37°C for 24 h. The Golgi apparatus in live MeWo cells was pulse-labeled for 30 min with BODIPY Texas Red-ceramide complexed with BSA (Molecular Probes, Inc.); cells were fixed, permeabilized with 2% paraformaldehyde in PBS with 0.05% Triton X-100, and stained with the anti-gE MAb 3B3 and FITC-conjugated anti-mouse IgG (Jackson Immunoresearch, Inc.) to visualize gE. The slides were mounted with ProLong antifade reagent (Molecular Probes, Inc.) for examination by confocal microscopy.

Western blot analysis. Protein lysates from cells infected with rOka or rOka-gE C-terminal mutant viruses were mixed with SDS sample buffer and boiled at 95°C for 5 min. Proteins were separated on an SDS–10% PAGE gel and transferred to a nitrocellulose membrane. The anti-gE MAb 3B3 was used at a dilution of 1:5,000 to 1:10,000 as the probe; it was detected with a horseradish peroxidase-conjugated donkey anti-mouse antibody (Amersham Inc., Little Chalfont, Buckinghamshire, United Kingdom) at a dilution of 1:3,000 to 1:5,000 and then visualized by ECL (Amersham).

Infection of skin and T-cell xenografts in SCIDhu mice. Skin and T-cell xenografts were made in homozygous CB-17$^{scid/scid}$ mice by using human fetal tissues obtained according to federal and state regulations, as described previously (24–27). Animal use was in accordance with the Animal Welfare Act and was approved by the Stanford University Administrative Panel on Laboratory Animal Care. rOka and rOka-gE C-terminal mutants were passed three times in primary HEL cells for inoculation of the xenografts; infectious virus titers were determined for each inoculum when the xenografts were injected. Skin xenografts were harvested after 14, 21, and 28 days, and T-cell xenografts were collected at 9 and 16 days, for analysis by infectious focus assay. Viruses recovered from implants were tested to confirm the ORF68 mutation by PCR and sequencing.

RESULTS

Effect of deleting the gE C terminus on VZV replication. As reported previously, the complete deletion of ORF68, which encodes gE, was incompatible with VZV replication (22). In these experiments, we evaluated whether the C terminus of gE was required for viral growth. Cosmids pvSpe21gEΔC-1 and pvSpe21gEΔC-2 had an ORF68 mutation that deleted the last 62 aa from the terminus of gE (aa 562 to 623). Cotransfection of each of the two separately derived pvSpe21gEΔC cosmids with pvSpe5, pvPme19, and pvFsp4 yielded no infectious virus. Cells transfected with the mutant cosmids were passed every 3 to 4 days for 28 days to ensure that delayed replication could be detected, and transfections with the two Spe21gEΔC cosmids and the intact VZV cosmids were repeated three times. Parallel transfections done with intact pvSpe21 and pvFsp4, pvSpe5, and pvPme19 were included as a positive control in all experiments. Infectious virus was recovered with intact VZV cosmids within 6 to 8 days after transfection.

Effects of targeted mutations in the YAGL, AYRV, and SSTT motifs of the gE C-terminal domain on VZV replication. Based on transient expression experiments, the endodomain of gE contains three functional motifs (Fig. 1A) that mediate the endocytosis of gE from the plasma membrane (YAGL), its trafficking to the TGN (AYRV), and C-terminal phosphorylation (SSTT) (17, 29, 42). Mutant cosmids pvSpe21gE-YAGL, pvSpe21gE-AYRV, and pvSpe21gE-SSTT, each with an ORF68 mutation of one of these three motifs, were constructed to evaluate effects on viral growth. Cotransfection of cosmids that contained mutations of the YAGL motif in the gE endodomain, along with pvSpe5, pvPme19, and pvFsp4, yielded no infectious virus. The transfections were done with two independently derived pvSpe21gE-YAGL mutants, which were tested three times each, with the same results. rOka was generated consistently in parallel transfections done with intact pvSpe21. These observations suggested that the gE endocytosis motif, YAGL, was essential for VZV replication.

To determine whether the YAGL mutation could be complemented by gE-expressing cell lines, experiments were done in which pGlowgE or Met-gE cells were transfected with pvSpe21gE-YAGL and the three intact cosmids. Transfection into pGlowgE cells yielded infectious virus in 2 weeks despite the disruption of the YAGL motif. Transfection of pvSpe21gE-YAGL, pvSpe5, pvPme19, and pvFsp4 into Met-gE cells resulted in detection of viral plaques after 4 weeks. PCR and sequencing confirmed that the alteration in nucleotides encoding the YAGL motif was present in the rOka-gE-YAGL mutants. rOka was also recovered when pGlowgE or Met-gE cells were transfected with the intact cosmids, indicating that gE expression by the cell lines did not inhibit viral replication.

In contrast to the pvSpe21gE-YAGL results, transfections of melanoma cells with pvSpe21gE-AYRV or pvSpe21gE-SSTT cosmids, along with pvSpe5, pvPme19, and pvFsp4, yielded infectious virus in all experiments. The resulting VZV recombinants, designated rOka-gE-AYRV and rOka-gE-SSTT, had the expected mutations, based on PCR screening and DNA sequencing (data not shown).

Growth kinetics of rOka-gE-AYRV and rOka-gE-SSTT recombinants in vitro. Analysis of the growth kinetics of rOka-gE-AYRV showed rapid spread compared to rOka and rOka-gE-SSTT during the first day after inoculation of MeWo cells in vitro (Fig. 1B). The peak titer of rOka-gE-AYRV at day 1 was equivalent to the peak titer of rOka, which was reached on day 3. In contrast, the rOka-gE-SSTT mutants grew to a significantly higher titer than rOka in MeWo cells on day 3 (Fig. 1B). After reaching peak levels, all strains showed a decrease in titer as the target MeWo cells were destroyed. These results suggest that alterations in gE localization to the TGN and phosphorylation of the C-terminal domain have effects on the spread and infectivity of VZV.

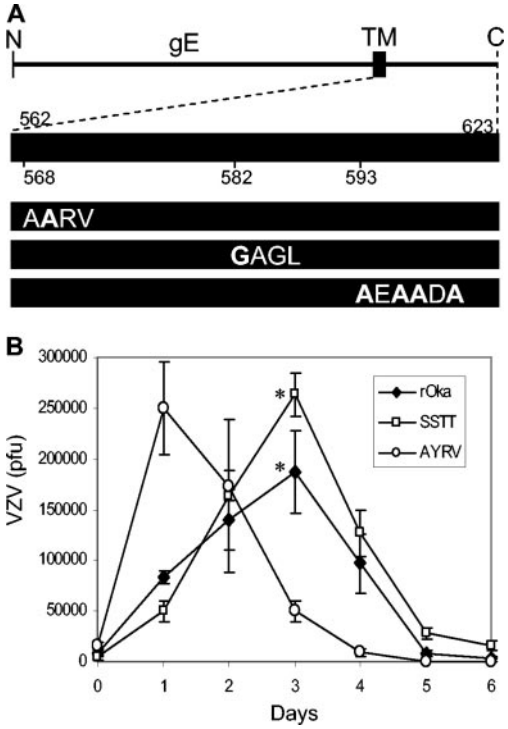

FIG. 1. Mutations of the gE C-terminal motifs YAGL, AYRV, and SSTT and their effects on VZV replication in vitro. (A) ORF68 encodes gE, a 623-aa type I membrane glycoprotein. The diagram shows gE, its transmembrane domain (TM), and the 62-aa C terminus. Mutations were made in the YAGL endocytosis motif; the AYRV motif, implicated in gE localization to the TGN; and serine/threonine residues that are targeted for phosphorylation (mutations in boldface type). (B) Yields of infectious virus were determined for 6 days after inoculation of MeWo cells with 8.3×10^3 PFU of rOka (diamonds), 1.5×10^4 PFU of rOka-gE-AYRV (circles), or 4.0×10^3 PFU of rOka-gE-SSTT (squares). Titer values represent the mean of triplicate samples for each time point. Error bars indicate the standard deviation; the significance (*) of differences between rOka and rOka-gE-SSTT on day 3 was determined by the paired, two-tailed Student t test ($P = 0.04$).

Localization of gE and plaque morphology of rOka-gE-AYRV and rOka-gE-SSTT recombinants in vitro. The apparent differences between the growth kinetics of the mutants and that of rOka could reflect changes in the localization of gE, which is involved in cell-cell spread when gE is associated with its partner gI. To monitor the expression and trafficking of gE, and to observe the extent of cell fusion, we performed confocal microscopy on MeWo cells stained for gE and the Golgi apparatus. To observe the effects of SSTT and AYRV mutations after approximately one full round of VZV replication, MeWo

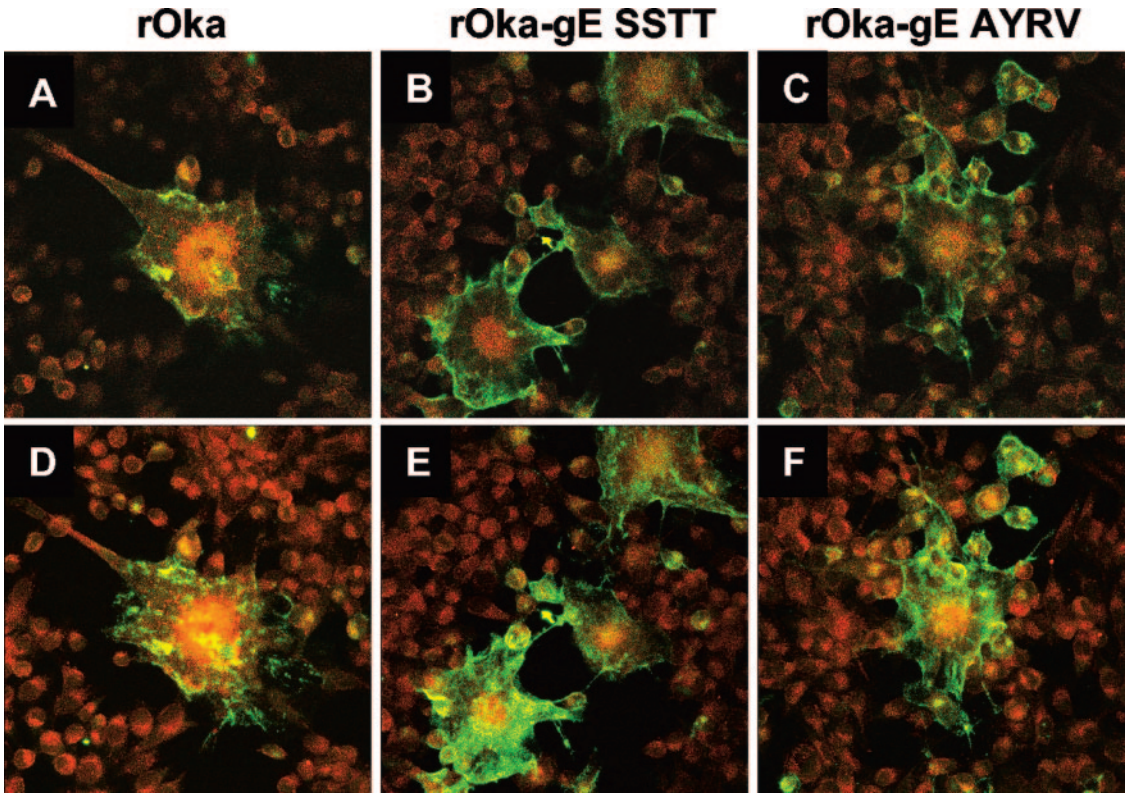

FIG. 2. Localization of gE in melanoma cells 24 h after infection with rOka or rOka gE C-terminal mutants. Melanoma cells were infected with rOka (left panels), rOka-gE-SSTT (center panels), or rOka-gE-AYRV (right panels) for 24 h, and then the Golgi apparatus in live melanoma cells was pulse-labeled for 30 min with BODIPY Texas Red-ceramide complexed with BSA. After fixation, gE was detected with MAb 3B3 and FITC-conjugated anti-mouse IgG by confocal microscopy. Merged images from a single central plane (A, B, C) and merged projections spanning the entire depth of the monolayer (D, E, F) were obtained by using Adobe Photoshop software. Magnification, ×40.

cells were infected for 24 h, treated with a monoclonal antibody to the N-terminal domain of gE (green) and the Golgi marker ceramide (red), and examined by confocal microscopy. Merged images from a single horizontal plane within the syncytia showed that the C-terminal mutant forms of gE were abundant on the surface (Fig. 2A to C), whereas wild-type gE was mainly intracellular and colocalized with the Golgi marker. Projections of merged images spanning the entire depth of the syncytia showed the increase in mutant gE levels on the plasma membrane (Fig. 2D to F). The increased localization of gE on the surfaces of MeWo cells infected with rOka-gE-AYRV and rOka-gE-SSTT offered an explanation for their increased spread and infectivity in the plaque assays.

To evaluate the localization of mutant gE and virus spread during the interval from 3 to 5 days, infected MeWo cells and Vero cells were collected after 72 h and analyzed by confocal microscopy (Fig. 3). MeWo cells are the standard cell type used for studying VZV protein trafficking, and Vero cells are African green monkey kidney cells that replicate VZV somewhat less efficiently and have revealed phenotypes of strains lacking gI (7). In these experiments, cells were stained with the anti-gE MAb (red) and ceramide (green). MeWo cells infected with rOka formed polykaryocytes with the usual regular arrangement of nuclei surrounding centralized Golgi structures (Fig. 3A, green). At this late time point, gE expression was abundant and was predominant along plasma membranes in cells infected with rOka or rOka-gE-SSTT (Fig. 3A and B, red). In contrast to rOka-infected cells, MeWo cells infected with rOka-gE-SSTT or rOka-gE-AYRV had disorganized patterns of TGN localization (Fig. 3B and C, green). Localization of gE was aberrant in MeWo cells infected with rOka-gE-AYRV, where gE had a much more punctate intracellular distribution (Fig. 3C). These different patterns of polykaryocyte formation, location of Golgi structures, and gE localization for melanoma cells infected with rOka, rOka-gE-SSTT, and rOka-gE-AYRV were not evident in Vero cells (Fig. 3D to F).

The intracellular localization of gE and the major immediate-early protein IE62 were also examined 72 h after infection of MeWo cells and Vero cells with rOka or gE C-terminal mutants. In these experiments, gE was stained with the anti-gE MAb (green) and IE62 was stained with a rabbit polyclonal antibody (red). As expected, expression of IE62 protein was abundant in MeWo cells examined 72 h after infection with rOka, and levels were similar in rOka-gE-SSTT- and rOka-gE-AYRV-infected cells (Fig. 4A to C). The nuclear expression of IE62 protein revealed the regular organization of nuclei in most rOka-infected polykaryocytes (Fig. 4A), which was disrupted in cells infected with rOka-gE-SSTT or rOka-gE-AYRV (Fig. 4B and C). Examination of infected Vero cells showed gE accumulation in perinuclear areas, suggesting possible ER retention of gE at 72 h after infection (Fig. 4D to F). No differences in IE62 localization were evident in Vero cells

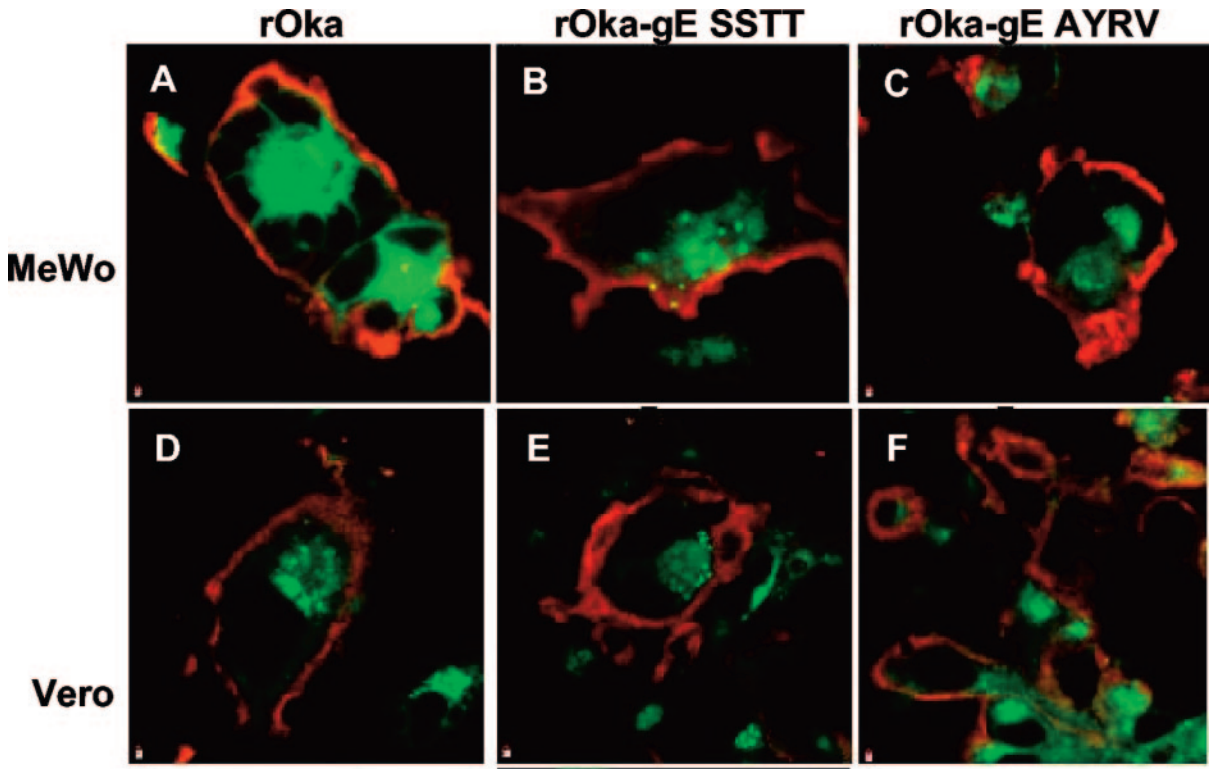

FIG. 3. Localization of gE and the Golgi apparatus in MeWo and Vero cells 72 h after infection with rOka or rOka gE C-terminal mutants. MeWo or Vero cells were infected with rOka (A, D), rOka-gE-SSTT (B, E), or rOka-gE-AYRV (C and F) for 72 h. Cells were examined by confocal microscopy for gE expression (red) by using the anti-gE MAb 3B3 and Texas Red-labeled goat anti-mouse IgG. The TGN was labeled with ceramide (green). Magnification, ×100.

infected with rOka or the gE C-terminal mutants (Fig. 4D to F). Taken together, these results point to dynamic changes in mutant gE localization in MeWo cells. At early times, both mutant forms of gE were found mainly on the plasma membrane. After 3 days, the Golgi complex was disorganized in cells infected with these mutants, while only gE-AYRV demonstrated punctate surface expression and increased intracellular localization. Abundant surface expression of gE-SSTT correlates with its growth advantage; similarly, reduced gE-AYRV expression at day 3 reflects its lower titer compared to those of rOka and rOka-gE-SSTT on the same day.

Effects of mutations of the C-terminal domain on posttranslational modification of gE. The apparent retention of gE in the ER or Golgi complex of infected Vero cells was intriguing. To further investigate the processing of gE in Vero cells, and the potential effects of the C-terminal mutations on gE maturation in MeWo cells, immunoblotting was performed. The mature form of gE made in infected cells is an O-linked and N-linked glycoprotein with a molecular weight of ~94,000 (~94K); the typical processing of gE results in predominance of this 94K mature form within 72 h (17, 28, 32). In these experiments, a broad band, ranging from 66 to 94K, with abundant signal at the higher molecular weight, was detected with the anti-gE MAb in MeWo cells infected with rOka, rOka-gE-SSTT, or rOka-gE-AYRV. No differences in the patterns of gE bands were observed with mutants expressing gE with C-terminal mutations, indicating that maturation was normal in MeWo cells (Fig. 5). Surprisingly, the predominant gE band was much smaller in Vero cells, ranging from 55 to 70K in cells infected with rOka. This unusual pattern of gE migration has not been observed before and suggests that gE maturation, for both rOka and the mutant strains, was substantially different in Vero cells than in human cells. However, the forms of gE detected in Vero cells infected with rOka-gE-SSTT or rOka-gE-AYRV at late times after inoculation did not differ from those present in rOka-infected cells (Fig. 5).

Effect of gE C-terminal mutations on VZV replication in skin and T-cell xenografts in SCIDhu mice. The growth kinetics of rOka and rOka-gE-SSTT in skin xenografts in SCIDhu mice were similar when evaluated at days 14, 21, and 28 after inoculation (Fig. 6A). As observed in MeWo cells infected in vitro, the titer of rOka-gE-SSTT was somewhat higher than that of rOka at the final time point. In contrast, the titers of infectious virus recovered from skin xenografts inoculated with rOka-gE-AYRV were significantly lower than those for rOka-gE-SSTT at 21 days, and lower than both those of rOka and rOka-gE-SSTT at 28 days ($P < 0.05$). In addition, 8 of 12 rOka-infected skin xenografts and 7 of 12 implants infected with rOka-gE-SSTT yielded infectious virus at 21 and 28 days, compared to only 4 of 12 implants infected with rOka-gE-AYRV. Recovery of infectious rOka virus from approximately 70% of skin xenografts is the typical pattern for this attenuated vaccine strain (26).

Growth of rOka-gE-AYRV was more restricted than growth of rOka and rOka-gE-SSTT in T-cell xenografts, based on peak titer ($P < 0.05$) (Fig. 6B). However, 89% of T-cell xenografts

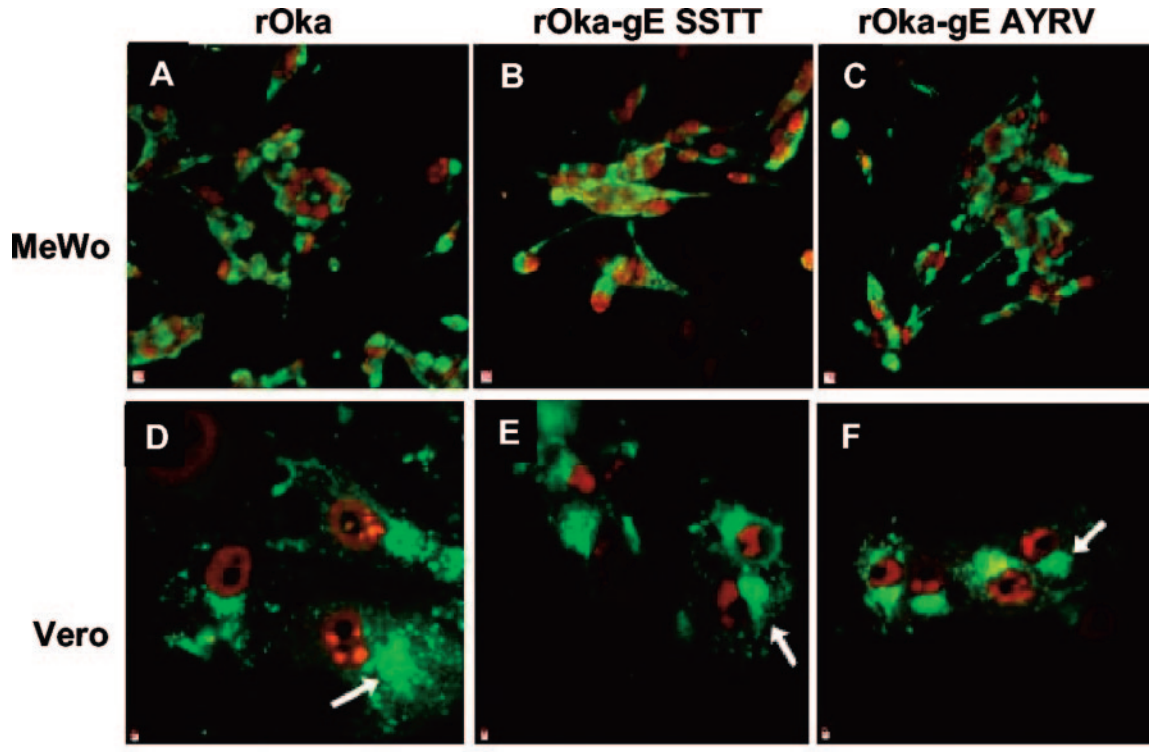

FIG. 4. Localization of gE and IE62 protein in MeWo and Vero cells 72 h after infection with rOka or rOka gE C-terminal mutants. MeWo or Vero cells were infected with rOka (A and D), rOka-gE-SSTT (B and E), or rOka-gE-AYRV (C and F) for 72 h. Cells were examined by confocal microscopy for gE expression (green) by using the anti-gE MAb 3B3 and FITC-labeled goat anti-mouse IgG. IE62 protein (red) was detected by using a rabbit anti-IE62 antiserum and Texas Red-labeled goat anti-rabbit IgG. Arrows indicate the accumulation of gE in intracellular vesicles. Magnification for A-C, ×40; magnification for D-F, ×100.

yielded some infectious rOka-gE-AYRV, including 5 of 5 implants harvested at day 9 and 3 of 4 implants tested at day 16. In contrast, rOka-gE-AYRV was recovered from only 33% (4 of 12) of skin xenografts. As was observed for T-cell xenografts inoculated with rOka, the titers of rOka-gE-SSTT had

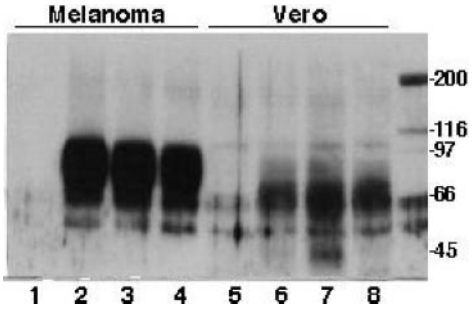

FIG. 5. Analysis of gE maturation in melanoma and Vero cells infected with rOka and gE C-terminal mutants. Melanoma cells were mock infected (lane 1) or inoculated with rOka (lane 2), rOka-gE-SSTT (lane 3), or rOka-gE-AYRV (lane 4) and harvested after 72 h. Cell lysates were separated by SDS–10% PAGE and transferred to a nitrocellulose membrane; the mouse anti-gE MAb 3B3 was used as the probe, the secondary antibody was anti-mouse IgG conjugated with horseradish peroxidase, and the proteins were visualized by ECL. In parallel experiments, Vero cells were either mock infected (lane 5) or inoculated with rOka (lane 6), rOka-gE-SSTT (lane 7), or rOka-gE-AYRV (lane 8) and harvested after 72 h. Molecular markers that were radiolabeled with ^{14}C are shown in the rightmost lane.

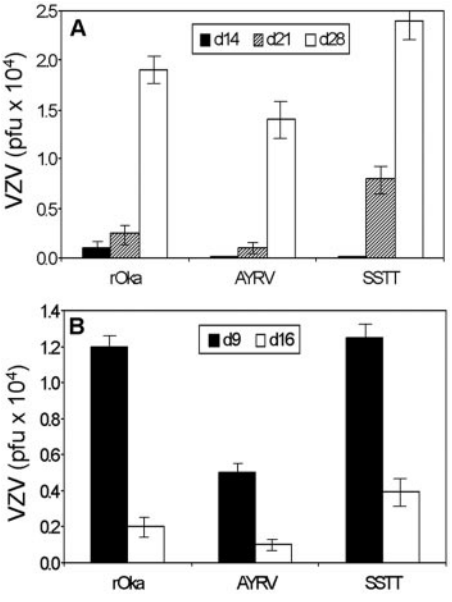

FIG. 6. Effects of mutations in the gE C terminus on VZV replication in skin and T-cell xenografts in SCIDhu mice. (A) Skin xenografts were inoculated with rOka or an rOka-gE-AYRV or rOka-gE-SSTT mutant. Each bar represents the mean titer of infectious virus recovered from skin implants harvested at day 14, 21, or 28 after inoculation; error bars indicate the standard error. (B) Mean titer of infectious virus found when T-cell xenografts were inoculated with rOka, rOka-gE-AYRV, or rOka-gE-SSTT and harvested at day 9 or 16 after infection. Inoculum titers were 2.5×10^4 to 7.0×10^4 PFU/ml. Significance was determined by Student's t test ($P < 0.05$).

declined by day 16, reflecting depletion of target cells at later time points associated with extensive VZV replication in T-cell implants. Sequencing showed that the original C-terminal mutations of gE were retained and compensatory mutations did not arise after replication of rOka-gE-AYRV and rOka-gE-SSTT in SCIDhu xenografts (data not shown).

DISCUSSION

In contrast to gE homologues in herpes simplex virus type 1 and pseudorabies virus, VZV gE is an essential glycoprotein (5, 11, 22, 37, 38). VZV gE expression on plasma membranes contributes to cell fusion, and gE is involved in virion assembly in the TGN, as indicated by the consequences of altered gE localization and defective virion formation when its heterodimer partner, gI, is deleted (9, 20, 21, 40). VZV gE is synthesized as a typical type I membrane glycoprotein, moving from the ER to the Golgi apparatus for posttranslational modification, followed by transfer to plasma membranes that form cell surfaces. This process is coupled with mechanisms for gE endocytosis from plasma membranes into endosomes, which transport gE back to the TGN for virion tegument assembly and envelopment (39, 42). Through these tandem mechanisms, gE concentrations in plasma membranes and the TGN are optimized to support both cell-cell spread and the assembly and envelopment of progeny virions.

This analysis of the functions of the gE C terminus in the context of the viral genome represents the first observations about how targeted mutations of this essential VZV glycoprotein affect viral replication in vitro, and how they affect VZV virulence in skin and T cells in vivo. A hierarchy was established in the requirement for each of the three functional motifs in the gE C terminus, which have been defined by transient expression experiments (17, 29, 42). First, the Y582G mutation was lethal for VZV replication, which accounts for our observation that the gE C terminus was essential. The YAGL residues (aa 582 to 585) mediate gE internalization from plasma membranes into early endosomes by interaction with the cellular adapter protein AP2 (30). The second motif, AYRV (aa 568 to 571), targets gE to the TGN (39, 42). Changing these residues to AARV had significant consequences, including failure to reorganize the Golgi apparatus in the typical VZV arrangement. Most importantly, the AYRV motif, while dispensable in vitro, was a determinant of VZV virulence, particularly in skin, and to a lesser extent in T cells, in vivo in the SCIDhu mouse model of VZV pathogenesis. Third, the SSTT acid patch comprises a consensus sequence for phosphorylation by VZV ORF47 protein kinase and the related cellular protein, casein kinase II (17). When gE was expressed from plasmids in MeWo cells, ORF47 phosphorylation of the serines and threonines favored gE trafficking to the TGN, while CKII phosphorylation, which targets threonines only, enhanced gE recycling to plasma membranes. In our experiments, replacement of these serines and threonines with alanine in the context of the VZV genome did not hinder VZV growth kinetics or plaque size in vitro, or infectivity in differentiated skin or T cells in vivo. In fact, the SSTT mutations resulted in higher peak titers, which is unprecedented in our experience with constructing recombinant viruses using the VZV cosmid system.

The observation that rOka-gE-SSTT exhibited somewhat enhanced replication is intriguing. Experiments with a naturally occurring variant, VZV-MSP, which has a gE mutation (D150N), demonstrated that altering gE, in this case in the N terminus, accelerated growth in vitro and was associated with more-extensive infection of skin xenografts (32). The rOka-gE-SSTT mutant shared this characteristic, confirming that replacement of only one or a few amino acids in gE may increase VZV infectivity in skin in vivo. In VZV-infected cells, gE is predominantly phosphorylated on serines, ORF47 kinase mediates most gE phosphorylation, and differential phosphorylation of the gE C-terminal SSTT motif directs gE to the TGN or back to plasma membranes (17, 28). The critical importance of ORF47 kinase activity is substantiated by the failure of CKII, which is abundant in human skin cells, to compensate for the absence of ORF47 kinase activity when skin xenografts were infected with ORF47ΔC or ORF47D-N kinase-defective mutants (6). However, our finding that rOka-gE-SSTT replicated as well as rOka in skin suggests that phosphorylation by ORF47 or CKII, or by other, unidentified kinases, was not required in this tissue. If the acid patch is important for tissue tropism, then the gE sorting mediated by differential phosphorylation of SSTT could be involved in VZV replication or latency in neurons, for example. It is also possible that when the acid patch was disrupted, other serines or threonines, of which there are seven in the endodomain, were phosphorylated and substituted functionally for the ORF47 and CKII sites. The impaired virulence of rOka-gE-AYRV, despite an intact acid patch, also indicates that the TGN signal is more important than SSTT for correct gE localization in differentiated cells in vivo.

VZV infection of skin requires cell-cell spread, which is likely to depend on the "fusion-from-within" functions of viral glycoproteins (9, 31). Infection of SCIDhu skin xenografts produces authentic virions as observed by electron microscopy, like those observed in biopsy specimens of varicella skin lesions, whereas many VZV virions in cultured cells are defective and cell-free virus is not made (3, 8, 26). These observations suggest important differences in VZV replication and assembly between in vitro systems and the pathogenesis of infection in vivo. In seeking links between the phenotypes of our VZV mutants in vitro and their characteristics in vivo, we find that mutants with mutations that cause a reduced plaque size in cell culture can be predicted to replicate poorly in skin xenografts, as shown with the ORF63 mutants rOka/ORF63rev[T171], rOka/ORF63rev[S181], and rOka/ORF63rev [S185] (4), or not at all, as demonstrated with rOkaΔgI and single-copy IE62 mutants (24, 33). There is some evidence that if cell fusion and basic steps in nucleocapsid formation occur, VZV may spread from cell to cell in vitro without forming fully enveloped virions, as suggested by experiments with rOkaΔgI and rOKAORF66S mutants (24, 27, 40). The extent to which this phenomenon permits cell-cell spread of VZV in differentiated human skin cells in vivo has not been established. Notably, whereas rOkaORF66S was as infectious as rOka in skin, rOkaΔgI was unable to replicate (24, 27). Although more gE was localized to punctate intracellular compartments at 72 h, some gE with the AYRV mutation reached plasma membranes at early and later times, which could allow cell fusion to occur. Thus, the limited capacity of rOka-gE-AYRV to infect skin may reflect cell-cell

spread of incompletely enveloped virions, according to the model proposed from in vitro experiments. Alternatively, sufficient gE may have localized to the TGN to permit assembly of small numbers of intact virions. Detection of gE in lysates from rOka-gE-AYRV-infected cells was not diminished compared to that for rOka, whereas gE synthesis was reduced in melanoma cells infected with the rOka-IE63 mutants. Both rOka-gE-AYRV and ORF63 mutants had substantially reduced infectivity in skin. Thus, these observations indicate that either altering gE trafficking by mutation of the TGN motif or decreasing overall gE synthesis resulted in attenuated VZV virulence in skin in vivo.

Aberrant polykaryocyte formation was observed in rOka-gE-AYRV- and rOka-gE-SSTT-infected cells, in a pattern that resembled the changes observed in MeWo cells infected with rOkaΔgI mutants compared to those infected with rOka (20). However, in contrast to a small-plaque phenotype, these experiments with gE C-terminal mutants indicate that formation of abnormal syncytia does not predict diminished VZV virulence in skin, since only rOka-gE-AYRV showed impaired cell-cell spread in skin in vivo. Vero cells infected with VZV showed increased accumulation of gE in perinuclear areas and faster migration on SDS-PAGE gels, which may indicate retention of mutant gE in the rough ER. It should also be noted that in Vero cells, VZV plaques are smaller and syncytia are less extensive than in MeWo cells, and this may contribute to differences in the amount of gE and its processing. Although gE has been implicated in recruiting IE62 and other tegument proteins to the TGN for virion assembly, the intracellular localization of IE62 protein was not different in MeWo or Vero cells infected with rOka-gE-AYRV versus rOka-gE-SSTT. As has been suggested with gI mutants, cytoplasmic IE62 concentrations may be too high to permit the detection of differences in TGN accumulation (40). It has been suggested that the binding of gE to gI might compensate for gE mutations affecting the TGN targeting signal, allowing gE to reach the TGN as part of the gE-gI complex (40). However, the experiments in which the AYRV signal was mutated in the context of the virus suggest that intact gI cannot replace the AYRV function sufficiently to permit typical VZV replication in vivo.

Our investigations with the SCIDhu model indicate that VZV infects CD4 and CD8 T cells in vivo without inducing cell fusion and polykaryocyte formation (25). Single VZV-infected cells are distributed throughout T-cell xenografts, and cell-free virus is detected, suggesting that enveloped virions are released and enter uninfected T cells by "fusion from without." Given these observations, T-cell infectivity would be predicted to be affected by mutations that interfere with envelopment and egress of intact, enveloped virions. We have found that a small-plaque phenotype in cell culture does not correlate with altered growth of VZV mutants in T-cell xenografts, as it does in skin. Small-plaque mutants may be unable to replicate in T cells, as observed with the ΔgI and single-copy IE62 mutants, or T-cell tropism may be unaffected, as observed with the IE63 mutants (4, 24, 33). Based on the model that the formation of complete virions is required for VZV T-cell tropism, the normal replication of IE63 mutants in T-cell xenografts suggested that the lower concentrations of gE made by these viruses remained adequate for virion assembly and envelopment. In the present experiments, rOka-gE-AYRV was less infectious in T-cell xenografts than rOka, even though gE expression in infected cells in vitro was not reduced. These observations suggest that gE concentrations can be diminished substantially without detrimental consequences for T-cell tropism but that AYRV-directed gE trafficking to the TGN for virion assembly is necessary for optimal VZV infection of T cells.

ACKNOWLEDGMENTS

This work was supported by grant AI20459 from the National Institute of Allergy and Infectious Diseases (to A.M.A). J.M. was supported by NRSA AI09195, and C.M. received a postdoctoral fellowship from the VZV Research Foundation.

REFERENCES

1. **Alconada, A., U. Bauer, L. Baudoux, J. Piette, and B. Hoflack.** 1998. Intracellular transport of the glycoproteins gE and gI of the varicella-zoster virus. gE accelerates the maturation of gI and determines its accumulation in the trans-Golgi network. J. Biol. Chem. **273:**13430–13436.
2. **Alconada, A., U. Bauer, and B. Hoflack.** 1996. A tyrosine-based motif and a casein kinase II phosphorylation site regulate the intracellular trafficking of the varicella-zoster virus glycoprotein I, a protein localized in the trans-Golgi network. EMBO J. **15:**6096–6110.
3. **Arvin, A. M.** 2001. Varicella-zoster virus, p. 2731–2768. *In* D. M. Knipe, P. M. Howley, D. E. Griffin, R. A. Lamb, M. A. Martin, B. Roizman, and S. E. Straus (ed.), Fields virology, 4th ed., vol. 2. Lippincott-Raven, Philadelphia, Pa.
4. **Baiker, A., C. Bagowski, H. Ito, M. Sommer, L. Zerboni, K. Fabel, J. Hay, W. Ruyechan, and A. M. Arvin.** 2004. The immediate-early 63 protein of varicella-zoster virus: analysis of functional domains required for replication in vitro and for T-cell and skin tropism in the SCIDhu model in vivo. J. Virol. **78:**1181–1194.
5. **Balan, P., N. Davis-Poynter, S. Bell, H. Atkinson, H. Browne, and T. Minson.** 1994. An analysis of the in vitro and in vivo phenotypes of mutants of herpes simplex virus type 1 lacking glycoproteins gG, gE, gI or the putative gJ. J. Gen. Virol. **75:**1245–1258.
6. **Besser, J., M. H. Sommer, L. Zerboni, C. P. Bagowski, H. Ito, J. Moffat, C. C. Ku, and A. M. Arvin.** 2003. Differentiation of varicella-zoster virus ORF47 protein kinase and IE62 protein binding domains and their contributions to replication in human skin xenografts in the SCID-hu mouse. J. Virol. **77:** 5964–5974.
7. **Cohen, J. I., and H. Nguyen.** 1997. Varicella-zoster virus glycoprotein I is essential for growth of virus in Vero cells. J. Virol. **71:**6913–6920.
8. **Cohen, J. I., and S. E. Straus.** 2001. Varicella-zoster virus and its replication, p. 2707–2730. *In* D. M. Knipe, P. M. Howley, D. E. Griffin, R. A. Lamb, M. A. Martin, B. Roizman, and S. E. Straus (ed.), Fields virology, 4th ed., vol. 2. Lippincott-Raven, Philadelphia, Pa.
9. **Cole, N. L., and C. Grose.** 2003. Membrane fusion mediated by herpesvirus glycoproteins: the paradigm of varicella-zoster virus. Rev. Med. Virol. **13:** 207–222.
10. **Davison, A. J., and J. E. Scott.** 1986. The complete DNA sequence of varicella-zoster virus. J. Gen. Virol. **67:**1759–1816.
11. **Dingwell, K. S., L. C. Doering, and D. C. Johnson.** 1995. Glycoproteins E and I facilitate neuron-to-neuron spread of herpes simplex virus. J. Virol. **69:** 7087–7098.
12. **Gershon, A., D. Sherman, Z. Zhu, C. Gabel, R. Ambron, and M. Gershon.** 1994. Intracellular transport of newly synthesized varicella-zoster virus: final envelopment in the trans-Golgi network. J. Virol. **68:**6372–6390.
13. **Grose, C.** 1980. The synthesis of glycoproteins in human melanoma cells infected with varicella-zoster virus. Virology **101:**1–9.
14. **Ito, H., M. H. Sommer, L. Zerboni, H. He, D. Boucaud, J. Hay, W. Ruyechan, and A. M. Arvin.** 2003. Promoter sequences of varicella-zoster virus glycoprotein I targeted by cellular transactivating factors Sp1 and USF determine virulence in skin and T cells in SCIDhu mice in vivo. J. Virol. **77:**489–498.
15. **Johnson, D. C., M. Webb, T. W. Wisner, and C. Brunetti.** 2001. Herpes simplex virus gE/gI sorts nascent virions to epithelial cell junctions, promoting virus spread. J. Virol. **75:**821–833.
16. **Kemble, G. W., P. Annunziato, O. Lungu, R. E. Winter, T. A. Cha, S. J. Silverstein, and R. R. Spaete.** 2000. Open reading frame S/L of varicella-zoster virus encodes a cytoplasmic protein expressed in infected cells. J. Virol. **74:**11311–11321.
17. **Kenyon, T. K., J. I. Cohen, and C. Grose.** 2002. Phosphorylation by the varicella-zoster virus ORF47 protein serine kinase determines whether endocytosed viral gE traffics to the trans-Golgi network or recycles to the cell membrane. J. Virol. **76:**10980–10993.
18. **Kimura, H., S. E. Straus, and R. K. Williams.** 1997. Varicella-zoster virus glycoproteins E and I expressed in insect cells form a heterodimer that requires the N-terminal domain of glycoprotein I. Virology **233:**382–391.
19. **Ku, C. C., J. A. Padilla, C. Grose, E. C. Butcher, and A. M. Arvin.** 2002. Tropism of varicella-zoster virus for human tonsillar $CD4^+$ T lymphocytes

that express activation, memory, and skin homing markers. J. Virol. **76:** 11425–11433.
20. **Mallory, S., M. Sommer, and A. M. Arvin.** 1997. Mutational analysis of the role of glycoprotein I in varicella-zoster virus replication and its effects on glycoprotein E conformation and trafficking. J. Virol. **71:**8279–8288.
21. **Maresova, L., T. J. Pasieka, and C. Grose.** 2001. Varicella-zoster virus gB and gE coexpression, but not gB or gE alone, leads to abundant fusion and syncytium formation equivalent to those from gH and gL coexpression. J. Virol. **75:**9483–9492.
22. **Mo, C., J. Lee, M. Sommer, C. Grose, and A. M. Arvin.** 2002. The requirement of varicella-zoster virus glycoprotein E (gE) for viral replication and effects of glycoprotein I on gE in melanoma cells. Virology **304:**176–186.
23. **Mo, C., E. E. Schneeberger, and A. M. Arvin.** 2000. Glycoprotein E of varicella-zoster virus enhances cell-cell contact in polarized epithelial cells. J. Virol. **74:**11377–11387.
24. **Moffat, J., H. Ito, M. Sommer, S. Taylor, and A. M. Arvin.** 2002. Glycoprotein I of varicella-zoster virus is required for viral replication in skin and T cells. J. Virol. **76:**8468–8471.
25. **Moffat, J. F., M. D. Stein, H. Kaneshima, and A. M. Arvin.** 1995. Tropism of varicella-zoster virus for human $CD4^+$ and $CD8^+$ T lymphocytes and epidermal cells in SCID-hu mice. J. Virol. **69:**5236–5242.
26. **Moffat, J. F., L. Zerboni, P. R. Kinchington, C. Grose, H. Kaneshima, and A. M. Arvin.** 1998. Attenuation of the vaccine Oka strain of varicella-zoster virus and role of glycoprotein C in alphaherpesvirus virulence demonstrated in the SCID-hu mouse. J. Virol. **72:**965–974.
27. **Moffat, J. F., L. Zerboni, M. H. Sommer, T. C. Heineman, J. I. Cohen, H. Kaneshima, and A. M. Arvin.** 1998. The ORF47 and ORF66 putative protein kinases of varicella-zoster virus determine tropism for human T cells and skin in the SCID-hu mouse. Proc. Natl. Acad. Sci. USA **95:**11969–11974.
28. **Montalvo, E. A., and C. Grose.** 1986. Varicella-zoster virus glycoprotein gpI is selectively phosphorylated by a virus-induced protein kinase. Proc. Natl. Acad. Sci. USA **83:**8967–8971.
29. **Olson, J. K., and C. Grose.** 1998. Complex formation facilitates endocytosis of the varicella-zoster virus gE:gI Fc receptor. J. Virol. **72:**1542–1551.
30. **Olson, J. K., and C. Grose.** 1997. Endocytosis and recycling of varicella-zoster virus Fc receptor glycoprotein gE: internalization mediated by a YXXL motif in the cytoplasmic tail. J. Virol. **71:**4042–4054.
31. **Roizman, B., and D. M. Knipe.** 2001. Herpes simplex viruses and their replication, p. 2399–2459. *In* D. M. Knipe, P. M. Howley, D. E. Griffin, R. A. Lamb, M. A. Martin, B. Roizman, and S. E. Straus (ed.), Fields virology, 4th ed., vol. 2. Lippincott-Raven, Philadelphia, Pa.
32. **Santos, R. A., C. C. Hatfield, N. L. Cole, J. A. Padilla, J. F. Moffat, A. M. Arvin, W. T. Ruyechan, J. Hay, and C. Grose.** 2000. Varicella-zoster virus gE escape mutant VZV-MSP exhibits an accelerated cell-to-cell spread phenotype in both infected cell cultures and SCID-hu mice. Virology **275:**306–317.
33. **Sato, B., H. Ito, S. Hinchliffe, M. H. Sommer, L. Zerboni, and A. M. Arvin.** 2003. Mutational analysis of open reading frames 62 and 71, encoding the varicella-zoster virus immediate-early transactivating protein, IE62, and effects on replication in vitro and in skin xenografts in the SCID-hu mouse in vivo. J. Virol. **77:**5607–5620.
34. **Sommer, M. H., E. Zagha, O. K. Serrano, C. C. Ku, L. Zerboni, A. Baiker, R. Santos, M. Spengler, J. Lynch, C. Grose, W. Ruyechan, J. Hay, and A. M. Arvin.** 2001. Mutational analysis of the repeated open reading frames, ORFs 63 and 70 and ORFs 64 and 69, of varicella-zoster virus. J. Virol. **75:**8224–8239.
35. **Soong, W., J. C. Schultz, A. C. Patera, M. H. Sommer, and J. I. Cohen.** 2000. Infection of human T lymphocytes with varicella-zoster virus: an analysis with viral mutants and clinical isolates. J. Virol. **74:**1864–1870.
36. **Taylor, S. L., P. R. Kinchington, A. Brooks, and J. F. Moffat.** 2004. Roscovitine, a cyclin dependent kinase inhibitor, prevents replication of varicella-zoster virus. J. Virol. **78:**2853–2862.
37. **Tirabassi, R. S., and L. W. Enquist.** 1999. Mutation of the YXXL endocytosis motif in the cytoplasmic tail of pseudorabies virus gE. J. Virol. **73:**2717–2728.
38. **Tirabassi, R. S., and L. W. Enquist.** 1998. Role of envelope protein gE endocytosis in the pseudorabies virus life cycle. J. Virol. **72:**4571–4579.
39. **Wang, Z.-H., M. D. Gershon, O. Lungu, Z. Zhu, and A. A. Gershon.** 2000. Trafficking of varicella-zoster virus glycoprotein gI: T338-dependent retention in the trans-Golgi network, secretion, and mannose 6-phosphate-inhibitable uptake of the ectodomain. J. Virol. **74:**6600–6613.
40. **Wang, Z.-H., M. D. Gershon, O. Lungu, Z. Zhu, S. Mallory, A. M. Arvin, and A. A. Gershon.** 2001. Essential role played by the C-terminal domain of glycoprotein I in envelopment of varicella-zoster virus in the trans-Golgi network: interactions of glycoproteins with tegument. J. Virol. **75:**323–340.
41. **Yao, Z., W. Jackson, and C. Grose.** 1993. Identification of the phosphorylation sequence in the cytoplasmic tail of the varicella-zoster virus Fc receptor glycoprotein gpI. J. Virol. **67:**4464–4473.
42. **Zhu, Z., Y. Hao, M. Gershon, R. Ambron, and A. Gershon.** 1996. Targeting of glycoprotein I (gE) of varicella-zoster virus to the trans-Golgi network by an AYRV sequence and an acidic amino acid-rich patch in the cytosolic domain of the molecule. J. Virol. **70:**6563–6575.